



# Nanofluid as Working fluid in Heat Pipe - an Experimental Investigation

<sup>1</sup>Shanmugaraja.T, <sup>2</sup>V.Sajith, <sup>3</sup>C.B.Sobhan

<sup>1</sup>Thakur College of Engineering and Technology Mumbai, India

<sup>2,3</sup>School of Nano Science and Technology National Institute of Technology Calicut, Kerala, India

Email: Shanmugaraja.86@gmail.com<sup>1</sup>, sajith@nitc.ac.in<sup>2</sup>, csobhan@nitc.ac.in<sup>3</sup>

**Abstract :** The heat pipe is considered to be an efficient heat transfer device due its high thermal conductance and high heat transfer coefficient. Heat pipe is generally classified based on the working fluid and the operating temperature for the purpose it is required. Heat pipe has got several applications, which includes heat recovery purpose in a solar water heating system. The performance of heat pipe depends on the thermo-physical properties of the working fluid, which basically determines the operational limits of the heat pipe. Present work mainly focuses on the possibility of use of nanofluid as working fluid in heat pipe for the performance improvement. The Al<sub>2</sub>O<sub>3</sub> nanoparticles has been added to water in different volume concentrations and the variation in the thermo-physical properties like thermal conductivity, surface tension, capillary pressure and dynamic viscosity were determined. Heat pipe has been designed for the solar water heater application and four heat pipes were fabricated, one for distilled water and three for the Al<sub>2</sub>O<sub>3</sub> nanofluid (0.01%, 0.05% and 0.1% volume concentration). Extensive experiments were done to compare the performance of three heat pipes, by varying the power input at the evaporator section and the condenser water temperature. It was observed that the heat pipe charged with the 0.05% and 0.1% vol Al<sub>2</sub>O<sub>3</sub> nanofluid has better performance than the heat pipe charged with 0.01% vol Al<sub>2</sub>O<sub>3</sub> nanofluid and distilled water. The thermal conductance and the effective thermal conductivity of the 0.05% Al<sub>2</sub>O<sub>3</sub> nanofluid charged heat pipe was found to be 1.3 and 1.35 times greater than the heat pipe charged with distilled water, respectively. Wick structure of the heat pipe, after experimentation, was characterized by means of Scanning Electron Microscope and deposition of Al<sub>2</sub>O<sub>3</sub> nanoparticle was found in the wick structure.

**Keywords :** Aluminium oxide nanoparticles, Nanofluid, Surface tension, Thermal conductivity

## I. INTRODUCTION

Heat pipe is the efficient heat transfer device used in electronic cooling, heat recovery system and spacecraft thermal management. Heat pipe is basically used to transfer heat from one end to other end with small temperature gradient. One of the interesting aspects is that it has high thermal conductance and high heat transfer coefficient than any other solid materials<sup>[1]</sup>. The idea of heat pipe was first proposed by Gaugler in 1942 and later Grover, Cotter and Erickson of Los Alamos

National Laboratory invented the unique heat transfer device referred by them as “Heat pipes”<sup>[2]</sup>. Heat pipe is capable of transporting heat at high rates over large distance nearly isothermally and it also can work against gravity. Since it is a two phase device its heat transfer rate is very high. Since heat pipes do not have any moving parts, they have exceptional reliability, with the additional benefit of completely passive operation. In the solar water heating system heat pipe can be used as heat recovery agent and the performance of heat pipe solar water system is higher than the other solar water heating system which uses thermosyphon or heat exchanger. The solar radiation is absorbed by the evaporator section and subsequently heat is transferred to the water, circulating in the condenser section. The suitable working fluid for heat pipe in case of solar water heating application is water. There are some limitations in heat pipe which affect the heat transfer rate such as capillary action limit, entrainment limit, sonic limit, boiling limit and viscous limit. The heat transfer performance and the limitation of heat pipe orientation depend on diameter, length and working fluid. One of the methods to improve the performance of heat pipe is to improve the heat transfer properties of the working fluid used in it. The thermo physical properties of the working fluid can be improved by the suspension of nanoparticles in it, i.e. by the use of nanofluids. But the main issue in the use of nanofluids as the base fluid, which will drastically affect the heat pipe performance. Hence it is advisable to use dilute working fluid in heat pipe is the trapping of nanoparticles in the wick, especially for high dosing of nanoparticles in nanofluids as working fluid in the heat pipe. Heat pipe are used in heat recovery purpose such as solar water heating system and the performance of this system can be improved by the modification of the thermo physical properties of the working fluid. Shukla et al. [3] experimentally investigated the effect of copper and silver nanoparticle suspended in water and charged inside the cylindrical copper heat pipe with a 19.5mm outer diameter and a 400 mm length and compared the results with the heat pipe charged with de-ionized water. The experiments were carried out for different heat inputs in the range of 100–250 W. The efficiency of the

heat pipe was found to be increased by 14% as compared with the heat pipe filled with the base fluid. Moreover, it was observed that an increase in the metal fraction in copper–water nanofluids lead to enhancement in thermal efficiency of the heat pipe. Mousa [4] studied experimentally the behavior of nanofluid to improve the performance of a circular heat pipe. In this investigation pure water and  $\text{Al}_2\text{O}_3$ - water based nanofluid were used as working fluids. An experimental setup was fabricated to investigate the performance of heat pipe under different operating conditions. The effect of filling ratio, volume fraction of nanoparticles in the base fluid, and heat input rate on the thermal resistance were investigated. Total thermal resistance of the heat pipe for pure water and  $\text{Al}_2\text{O}_3$ -water based nanofluid was also predicted. An experimental correlation was obtained to predict the influence of prandtl number and dimensionless heat transfer,  $K_q$  on thermal resistance. It was also observed that thermal resistance decreases with increase in the concentration of  $\text{Al}_2\text{O}_3$ -water based nanofluids, as compared to that of pure water. Kang et al. [5] carried out experiments on a 1 mm thickness sintered circular heat pipe using silver nanofluid and pure water as working fluid. The experiments were performed for measuring the temperature distribution and comparing them for the nanofluid and DI-water. The test was carried out for different concentration of nanoparticle with size ranging from 10 to 35 nm, for different dosing level of 1, 10 and 100 mg/l. It was found that for the nanofluid charged heat pipe the temperature difference decreased by about 0.56 - 0.65 °C as compared to that of DI-water, for an input power of 30 - 50 W. It was also observed that the effect of size of nanoparticles on the thermal performance was low. Kang et al. also performed the experimental work [6] on grooved circular heat pipe with silver nanoparticle. It was demonstrated that the thermal resistance of the nanofluid filled heat pipe decreased upto 10 - 80% as compared to DI-water, for an input power of 30 - 60 W. The measured results also show that the thermal resistances of the heat pipe decreases as the silver nanoparticle size and concentration increase. Hyung et al. [7] carried out experimental investigation on circular screen mesh wick heat pipes using water-based  $\text{Al}_2\text{O}_3$  nanofluids with the volume fraction of 1.0 and 3.0 Vol.%. In their studies the wall temperature distributions and the thermal resistances between the evaporator and the adiabatic sections were measured and compared with those for the heat pipe using DI water. The averaged evaporator wall temperatures of the heat pipes using the water-based  $\text{Al}_2\text{O}_3$  nanofluids were observed to be much lower than those of the heat pipe using DI water. The thermal resistance of the heat pipe using the water-based  $\text{Al}_2\text{O}_3$  nanofluids with the volume fraction of 3.0 vol% was significantly reduced by about 40% at the evaporator-adiabatic section. A thin porous coating layer formed by nanoparticles suspended in nanofluids was observed in the wick structures. Based on this fact, they concluded that the primary mechanism of enhancement of thermal performance of heat pipe is mainly due to the

coating layer formed by nanoparticles at the evaporator section, as the layer not only extend the evaporation surface but also improve the surface wettability and capillary wicking performance. Liu et al. [8] reported the results from experimental investigation on the effect of aqueous CuO nanofluids on thermal performance of a horizontal mesh heat pipe, working at steady sub-atmospheric pressures. The experimental results shows that the addition of CuO nanoparticles (average diameter - 50 nm) in deionized water significantly enhances the heat transfer coefficients of both evaporator and condenser, and the maximum heat flux of the heat pipe. It was also observed that the heat transfer enhancement effects were found to be increase with the decrease in the operating pressure. The experimental results show that the thermal performance of a mesh heat pipe can be evidently strengthened by the use of CuO nanofluids instead of deionized water. Shafahi et al. [9] analytically studied the thermal performance of rectangular and disk-shaped heat pipes charged with nanofluids. In their analysis, they obtained the liquid pressure and velocity profile, temperature distribution of the heat pipe wall, temperature gradient along the heat pipe, thermal resistance and maximum heat load etc, for the flat-shaped heat pipes, utilizing nanofluid as the working fluid. The thermal performance of flat-shaped heat pipe was substantially enhanced with the use of nanofluid. The nanoparticles presence within the working fluid results in the decrease of thermal resistance and an increase in the maximum heat load capacity of the flat-shaped heat pipe. The optimum nanoparticle concentration level and wick thickness for maximum heat removal capability of the flat-shaped heat pipe was also determined. Huminc et al. [10] experimentally investigated the application of iron oxide nanoparticles in water, for the improvement of the thermal performance of a thermosyphon heat pipe. The main aim of the experiment was to compare the heat transfer rate of the thermosyphon heat pipe with nanofluid and DI-water, from the temperature distribution. Dosing level of nanoparticles was varied from 0 to 5.3% by (volume). As the inclination angle of heat pipe charged with nanofluid increases, the heat transfer also increases. The thermal resistance of the thermosyphon heat pipes with nanoparticle solution was observed to be lower than that with DI-water and also the thermal resistance decreases as the concentration of nano particles increases. Azad [11] studied the performance of heat pipe solar collector, theoretically and experimentally. The heat pipe solar collector consists of wick-assisted heat pipe, made of copper, for the heat transfer from the absorber (evaporator) to a heat exchanger (condenser). The theoretical model predicted the outlet water from heat exchanger, heat pipe temperature and also the thermal efficiency of solar collector. Simulated values of heat flux, heat pipe temperature, water outlet temperature and efficiency were found in good agreement with experimental results. Chaudhry et al. [12] reviewed the use of heat pipe systems in building and ground applications including heat recovery and renewable

energy application. The basic features, limitations and theoretical comparisons drawn with respect to the operating temperature profiles for the industrial systems were outlined. Working fluids for heat pipe were also compared on the basis of the figure of merit for the range of temperatures. The review established that standard tubular heat pipe systems present the largest operating temperature range in comparison to other systems and therefore offer viable potential for optimization and integration into renewable energy systems. Lin Lu et al. [13] carried out an investigation on the thermal performance of the open thermosyphon using respectively the deionized water and water-based CuO nanofluids as the working liquid. The effects of filling rate, type of the base fluid, nanoparticle mass concentration and the operating temperature on the heat transfer characteristics were discussed. From the experiment results they observed that optimum filling ratio in the evaporator is 60% and also the thermal performance of the open thermosyphon increase with the increase in the operating temperature. Water-based CuO nanofluids significantly enhance the thermal performance of the evaporator and evaporating heat transfer coefficients was observed to be increase by about 30% as compared to deionized water. The CuO nanoparticles mass concentration has remarkable influence on the heat transfer coefficient in the evaporation section and the mass concentration of 1.2% by (weight) corresponds to the optimal heat transfer enhancement. Hajian et al. [14] experimentally investigated the effect of nanofluid on the thermal performance of a medium-sized cylindrical meshed heat pipe, in both transient and steady states, by analyzing the thermal resistance and response time of the heat pipe. Nanofluid was prepared by suspending silver nanoparticles (at concentrations of 50, 200 and 600 ppm) in DI water. Nanofluid with low concentration was reported to give best performance and they also discussed the negative effects of high concentration nanofluids. It was also observed that thermal resistance and response time of the heat pipe decreased up to 30% and 20%, respectively for nanofluids, as compared to DI-water. From the literature it has been observed that the many researchers have used different nanofluid for improving the performance of heat pipe and some have used  $\text{Al}_2\text{O}_3$  nanofluids in heat pipe of high concentration. The present work aims at the experimental investigation on the possibility of use of dilute nano fluids as working fluid in heat pipes, which is used for the solar applications. Distillation procedure was used to prepare the dilute nanofluid and to estimate the maximum amount of nanoparticles carried along with the vapour. Various thermo physical properties of the dilute nanofluid were determined using the standard apparatus. The heat pipe was fabricated and charged with different concentration of dilute nano fluids. Experiments were conducted and heat transfer performance of heat pipe charged with dilute nano fluids was compared with that charged with water. The wick of the heat pipe charged with dilute nanofluid was later

analysed using SEM to investigate on the trapping of nanoparticles in the wick.

## II. EXPERIMENTATION

The methodology and experimental procedure used in the present work are explained in this chapter. Standard test methods were employed for determining different thermo physical properties of the distilled water and nanofluid of different concentration. Distillation of nanofluid has been done and the optical method has been used to determine the concentration of distillate fluid. Permeability of the wick structure has been determined. Experiments were performed on the different heat pipes for determining the performance and the procedure adopted is also presented in this chapter.

### 2.1 Synthesis of Nano fluid

Samples of Aluminium oxide nanoparticles of size 40 to 50 nano meters and density 4 g/ml were used as the additive in the distilled water. The dosing level of Aluminium oxide (by volume) in the base fluid was varied from 0.01% to 0.1% by volume. The required quantity of nanoparticles for each dosing level was measured using a precision electronic balance. Nanofluid was prepared by using a standard ultrasonic shaker, applying a constant agitation time. In the present study, the agitation time for preparing the nanofluid was 60 minutes. The nanofluid sample was used in the experiments immediately after preparation, without providing considerable time for sedimentation to set in. Fig.1.1 shows the nanofluid of different concentration synthesised for the experimentation.



Fig.1.1. Aluminium oxide nanofluid of concentration.

#### 1.1.1 Specifications of Ultrasonic shaker

Power	: 60 W
Capacity	: 2 litres
Operating frequency	: 33 kHz

### 2.2. Thermo physical properties of Working fluid

The performance of the heat pipe depends on various thermophysical properties of the working fluids. The properties measured in the present work include surface tension, contact angle thermal conductivity and dynamic viscosity and were measured using standard test methods. Surface tension of the distilled water and  $\text{Al}_2\text{O}_3$  nanofluid were measured using capillary rise

method. Contact angle of distilled water and  $\text{Al}_2\text{O}_3$  nanofluid was determined using standard optical techniques. Thermal conductivity of distilled water and  $\text{Al}_2\text{O}_3$  nanofluid was measured using KD2 Pro Analyser. Dynamic viscosity of distilled water and  $\text{Al}_2\text{O}_3$  nanofluid were determined by means of Brookfield Rheometer.

### 2.2.1 Surface tension

The surface tension was estimated for distilled water and various concentration of 0.01%, 0.05% and 0.1% volume of  $\text{Al}_2\text{O}_3$  nanofluid using Capillary rise method, as schematically shown in fig.1.2. The experiment was conducted for different temperature and temperature of the fluid was changed by means of a heater. The capillary rise ( $h$ ) was measured using a travelling microscope as shown in fig.1.3 and the contact angle ( $\theta$ ) was measured by means of a Stereo Zoom microscope as shown in fig.1.4. The magnified images were captured by a CCD camera (Fig.1.5) and further processed by MATLAB 7.0 software. An edge detection algorithm, which uses sobel approximation, was used to obtain the edges of the image captured, for estimating the contact angle. Edge detection algorithm return the edges of the image at the points where the intensity gradient is high and contact angle was then estimated using Motic Images Plus 2.0 ML software.

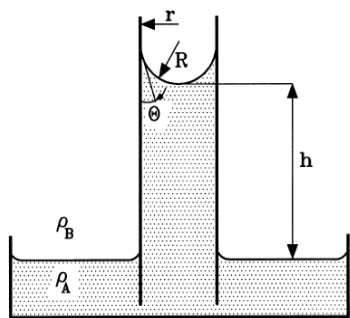


Fig.1.2.Capillary rise method<sup>[1]</sup>



Fig.1.3.Travelling microscope for capillary rise measurement

### 2.2.2 Contact angle

Contact angle of the fluid with the wick structure is a measure of its wettability and was measured by means of a Stereo Zoom microscope. The wick is made of copper material and as the measurement of contact angle on wick is found to be difficult, contact angle measurement was done on a copper plate of dimensions 1 cm x 1 cm x 1 mm. A droplet of distilled water was

injected onto the surface using a syringe pump and the advancing contact angle was measured by means of a Stereo Zoom microscope as shown in fig.1.6. Experiment was conducted for three different concentrations of  $\text{Al}_2\text{O}_3$  nanofluid. Magnified images were grabbed by means of a CCD



Fig.1.4.Stereo Zoom microscope for contact angle measurement

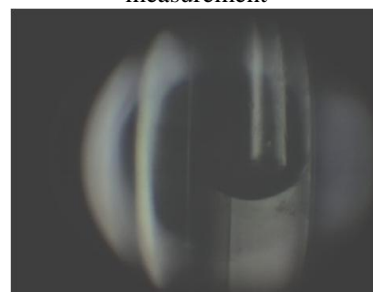


Fig.1.5.Microscope image of capillary tube with distilled water.

camera shown in fig.1.7 and were processed by MATLAB 7.0 software to obtain the contact angle, as explained earlier. The final reading was obtained by averaging out the reading of five droplets at different positions on the copper plate.

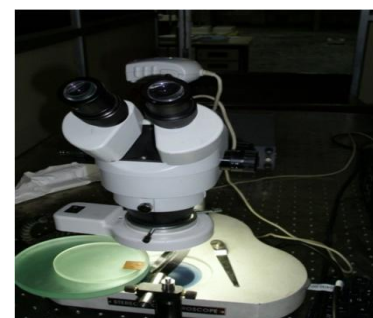


Fig.1.6.Experimental setup for contact angle measurement



Fig.1.7. Image of 0.01%  $\text{Al}_2\text{O}_3$  Nanofluid angle droplet on copper plate



### 2.2.3. Thermal conductivity

Thermal conductivity of nanofluids was measured by means of KD2 Pro Analyser, as shown in the fig.1.8. The instrument basically consists of a handheld controller and sensor that can be inserted into the medium for which property has to be measured. The KD2 Pro uses transient line heat source method for the measurement of thermal conductivity and resistivity and probe consists of a needle with a heater and temperature sensor inside. Current is passed through the heater and the temperature of the probe is monitored over time. From the analysis of the variation of the probe temperature with the time, the thermal conductivity is estimated. In order to maintain the temperature, the sample was kept in the constant temperature bath and thermal conductivity was determined at constant temperature.



Fig.1.8. Setup for thermal conductivity measurement

### 2.2.4 Dynamic viscosity

Viscosity is a measure of the resistance of a fluid which is being deformed by either shear or tensile stress. Dynamic viscosity of distilled water and various concentration of 0.01%, 0.05% and 0.1% volume of  $\text{Al}_2\text{O}_3$  nanofluid was measured by means of Brookfield DV-III Programmable Rheometer, as shown in fig.1.9, which measures fluid parameters of shear stress and viscosity at given shear rates. In a Rheometer, a spindle which is immersed in the test fluid, is driven through a calibrated spring and the viscous drag of the fluid against the spindle is estimated from spring deflection, which is measured by means of a rotary transducer. The required amount of sample is taken in the cup and the temperature of the sample is kept constant with the help of constant temperature bath. The speed of rotation of the spindle is adjusted until the steady viscosity value is attained and the readings were taken at different temperatures.

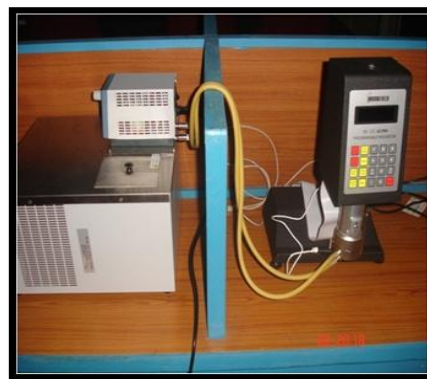


Fig.1.9. Brookfield DV-III Programmable Rheometer

### 2.3 Wick permeability

Permeability is the ability of the wick structure to allow the fluid through it and is determined by the Darcy's law. Darcy's law is a simple proportional relationship between the instantaneous discharge rate through a porous medium, the viscosity of the fluid and the pressure drop over a given distance.

$$Q = - \frac{KA(P_2 - P_1)}{\mu l \cdot L} \quad (1.1)$$

The total discharge,  $Q \text{ m}^3/\text{s}$  is equal to the product of the permeability of the medium,  $k \text{ (m}^2\text{)}$ , the cross-sectional area to flow,  $A \text{ m}^2$ , and the pressure drop ( $P_2 - P_1$ ), all divided by the viscosity,  $\mu \text{ (Pa.s)}$  and the length over which the pressure drop is taking place. The negative sign is needed due to the direction of fluid flow. Fig.1.10 shows the experimental setup for measurement of permeability. Test set up consists of two copper pipes of 19 mm diameter and 150 mm length, with pressure gauges attached on them and a wick of single layer of 100 meshes per inch is placed in vertical position between the tubes. The copper pipes were joined by placing the wick in between them with the help of washer, and sealed in such a way to avoid leakage. The water and  $\text{Al}_2\text{O}_3$  nanofluid of 0.01% vol were circulated through this setup with the help of  $\frac{1}{2}$  HP pump and the flow rate was maintained constant throughout the experiment. The pressure difference in the pressure gauge was noted after attaining steady state condition.

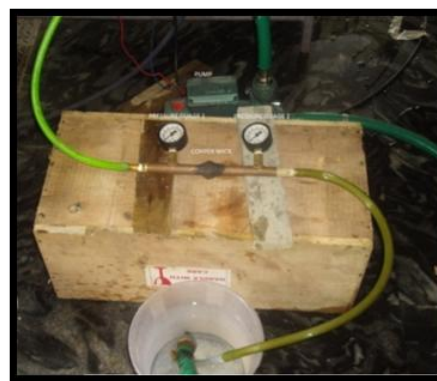


Fig.1.10. Setup for permeability measurement

## 2.4. Performance study of Heat pipe

The experiments were carried with the heat pipe charged with distilled water and nano fluids of 3 different concentrations ranging from 0.01% to 0.1% vol. Fig 1.11 shows the hat pipe charged with distilled water and the nanofluids of different concentrations. The experimental setup consists of a resistance band wire heater (maximum power output of 500 W), a watt meter, and an auto transformer as shown in fig.1.12. Seven thermocouples of the T type were fixed at different position of the heat pipe in the axial direction and was connected to the Data acquisition system (Make: Agilent 39470A) for simultaneous recording of the temperatures.

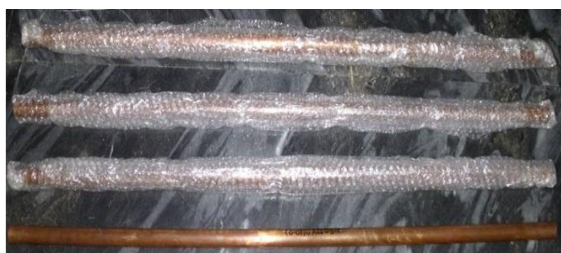


Fig.1.11. Heat pipes charged with water and  $\text{Al}_2\text{O}_3$  nanofluid

Four thermocouples were fixed in the evaporator section and three in condenser section. The inlet and outlet temperatures of the cooling water were measured using two T-type thermocouples. The flow rate of the cooling water circulating by constant temperature bath was measured by measuring jar and the flow rate was measured to be 0.05 kg/s, under steady

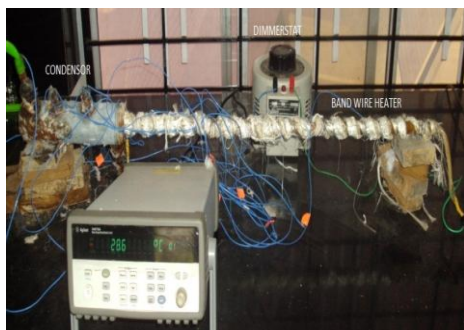


Fig.1.12. Heat pipe wrapped with wire band heater

state condition. The heat pipe with base fluids and nanofluids were tested for heat inputs varying from 80 to 120 W. Proper insulation was applied in the evaporator section. The heat input was varied by means of variable transformer from 80 to 120 W. The readings were taken with and without circulating the water to the condenser. The temperature at different positions of the heat pipe was monitored by the data acquisition unit once the steady state is attained.

## III. RESULTS AND DISCUSSION

### 3.1 Introduction

This chapter discusses the experimental results of the properties of working fluids used in the heat pipe. The results obtained for the properties of the wick structure

have been discussed. The results of the experiments carried out to compare the performance of the heat pipe, charged with water and nanofluids, are presented in details.

### 3.2 Working fluid properties

This section discusses the result obtained from the experimental investigation of the properties of the distilled water and  $\text{Al}_2\text{O}_3$  nanofluids.

#### 3.2.1 Surface tension

Surface tension of the distilled water and nanofluids was measured by means Capillary rise method, by measuring the contact angle and the capillary rise. Fig.1.13 shows the contact angle of distilled water in capillary tube. Significant change was not observed in the contact angle with the increase in the concentration of nanoparticles, as measured with capillary tube. The surface tension of the  $\text{Al}_2\text{O}_3$  nanofluids was found to be increased as compared with distilled water as shown in fig 1.14. The surface tension of the  $\text{Al}_2\text{O}_3$  nanofluids increases with the increase in concentration and decreases with the increase in the temperature. The nanoparticles added in the distilled water increases the density and enhance the particle-particle, particle-solid and particle-fluid interactions[15]. The operating limits of heat pipe such as capillary limit, entrainment limit and the boiling limit depends on the surface tension of the working fluid. As the surface tension of the  $\text{Al}_2\text{O}_3$  nanofluids is higher as compared with the distilled water, all the operational limits values of heat pipe such as capillary limit, entrainment limit and boiling limit will increase, by the use of nanofluids as working fluid in heat pipes.



Fig.1.13. Contact angle result of distilled water capillary tube

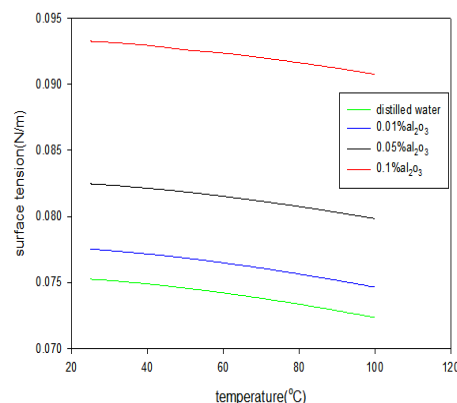


Fig.1.14. Variation of surface tension with temperature

### 3.2.2 Thermal conductivity

The thermal conductivity of the Al<sub>2</sub>O<sub>3</sub> nanofluids was measured by means of KD2Pro Analyser. The thermal conductivity of nanofluids was observed to be increasing with the nanoparticle concentration as shown in Fig.1.15. The reasons for the enhancement of thermal conductivity of nanofluids includes the Brownian motion of nanoparticles, liquid layering around nanoparticles, nature of the heat transport in the nanoparticles and Clustering of nanoparticles[15]. The increase in the thermal conductivity improves the thermal performance of heat pipe and also will affect the boiling limit of the heat pipe. The effective thermal conductivity of the wick structure increases as it depends on the thermal conductivity of wick material and the working fluid. The increase in the effective thermal conductivity of the wick structure in

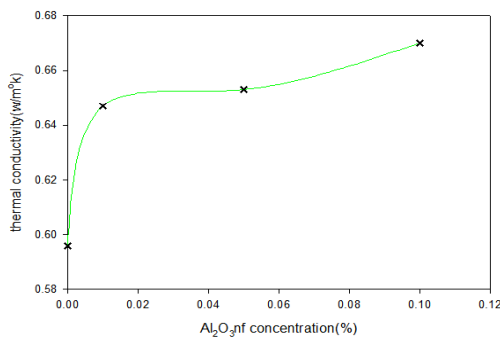


Fig.1.15. variation of thermal conductivities with concentration turn will lead to the increase in the boiling limit of the heat pipe.

### 3.2.3 Dynamic viscosity

The dynamic viscosity of the Al<sub>2</sub>O<sub>3</sub> nanofluids increases with the increases in concentration and found to decrease with the temperature as shown in fig.1.16. The nanoparticle added in the water increases the resistance between the layers of the fluid and hence increases the viscosity of the water. The capillary limit of the heat pipe depends on the liquid pressure drop in the heat pipe and viscosity will affect the liquid pressure drop in the heat pipe. Increase in viscosity of Al<sub>2</sub>O<sub>3</sub> nanofluids will increase the liquid pressure drop in the heat pipe, which in turn decreases the capillary limit of the heat pipe.

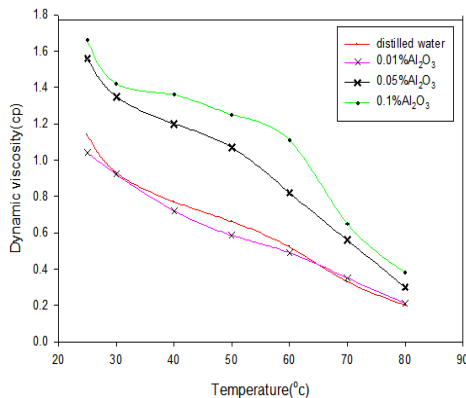


Fig.1.16. variation of viscosities with temperature

### 3.3 Wick properties

This section describes the experimental results of the capillary pressure and the permeability of the wick properties.

#### 3.3.1 Capillary pressure

When two immiscible fluids are in contact in the interstices of a wick, a discontinuity in pressure exists across the interface separating them. The difference in pressure  $P_c$  is called capillary pressure, which is pressure in the non-wetting phase minus the pressure in the wetting phase. The capillary pressure is given by,

$$P_c = \frac{2\sigma \cos(\theta)}{r_p} \quad (1.2)$$

The capillary pressure depends on the surface tension of the fluid and the contact angle of the fluid with the wick structure. As shown in the fig.1.17 the contact angle of 0.1% volume of Al<sub>2</sub>O<sub>3</sub> nanofluid with the copper plate is found to be 49.8°. The contact angle increases as the concentration increases as shown in fig.1.18.

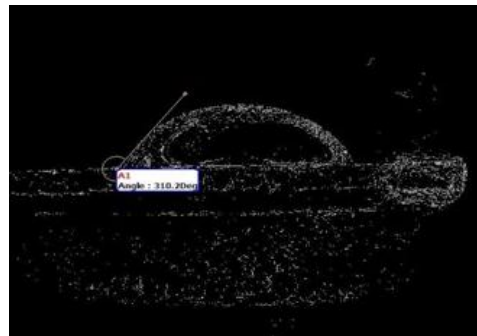


Fig.1.17 contact angle result of 0.1% nanofluid concentration

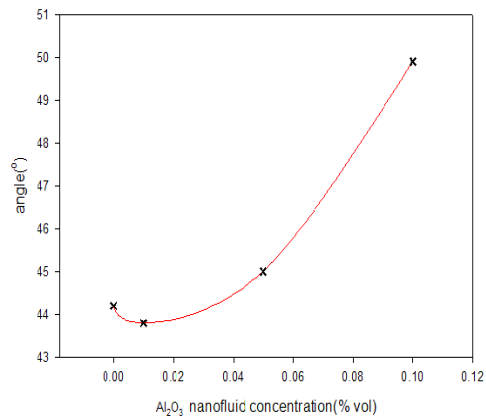


Fig.1.18. variation of contact angle with Al<sub>2</sub>O<sub>3</sub> nanofluid concentration

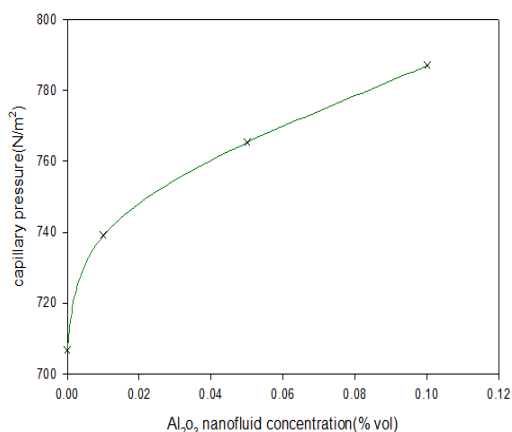


Fig.1.19. variation of capillary pressure with the concentration.

The capillary pressure of the Al<sub>2</sub>O<sub>3</sub> nanofluid increases with the concentration as shown in fig.1.19 and this will improve the capillary action of the wick structure compared with the distilled water. The capillary limit of the heat pipe charged with Al<sub>2</sub>O<sub>3</sub> nanofluid increases due to increase in capillary pressure.

### 3.3.2 Permeability

The permeability of the wick structure was found to be decreased for Al<sub>2</sub>O<sub>3</sub> nanofluid. The permeability with the distilled water and 0.01% Al<sub>2</sub>O<sub>3</sub> nanofluid was found to be  $1.057 \times 10^{-12} \text{ m}^2$  and  $7.93 \times 10^{-13} \text{ m}^2$  respectively and further decreases with increase in the nanoparticle concentration. The decrease in permeability will affect the flow of nanofluid inside the wick structure. This will also increase the liquid pressure drop inside the heat pipe, lowering the capillary limit.

### 3.4. Heat pipe experimental results

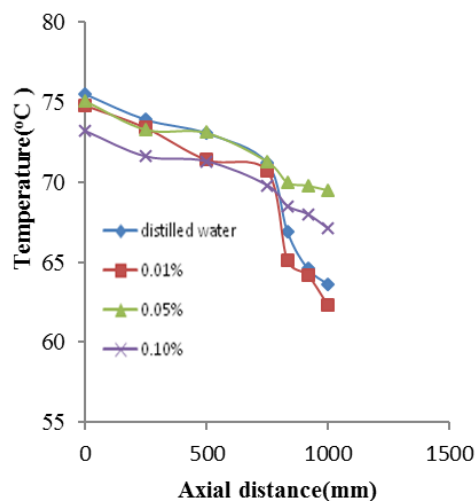
Experiments were conducted by charging the heat pipe with distilled water and also different concentrations of dilute nanofluids and temperature distribution was obtained along the length of the heat pipe, after attaining the steady state condition. Thermal conductance and the Effective thermal conductivity were estimated from the temperature profile and the heat input at the evaporator section.

#### 3.4.1. Surface temperature distribution profile

The surface temperature distribution along the length of the heat pipe was obtained for two cases, i.e. with air and water, as cooling medium in the condenser section and power input at the evaporator section was varied from 80 to 120 W.

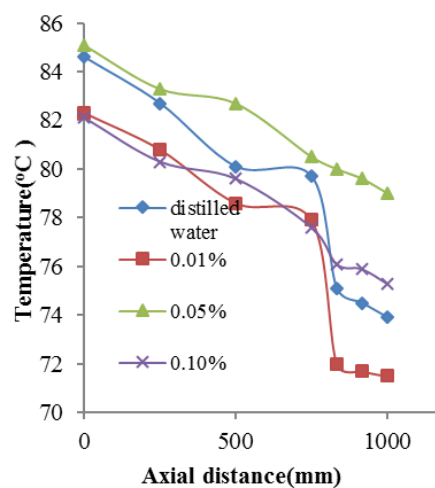
##### 3.4.1.1. Air as cooling medium

Experiments were conducted without circulating water through the condenser section. The surface temperature distribution profile along the heat pipe charged with distilled water and three different concentrations of Al<sub>2</sub>O<sub>3</sub> nanofluid is shown in the fig.1.20, for a power input of 80W.

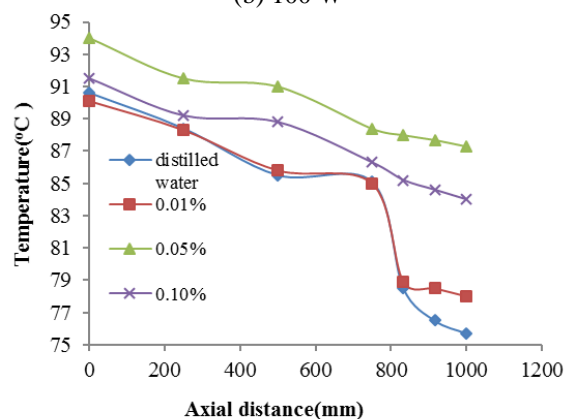


(a) 80 W

The temperature distribution profile for the power input of 100 W and 120 W are shown in the fig.1.20. From the result it was found that the heat pipe charged with the 0.05% and 0.1% vol Al<sub>2</sub>O<sub>3</sub> nanofluid has low temperature drop between the ends of the heat pipe. So, the heat pipe charged



(b) 100 W



(c) 120 W

Fig.1.20. Variation of surface temperature distribution along the heat pipe for the different power input without circulating the water to the condenser.



with the 0.05% and 0.1% vol Al<sub>2</sub>O<sub>3</sub> nanofluid has good performance than the heat pipe charged with distilled water and 0.01% vol Al<sub>2</sub>O<sub>3</sub> nanofluid.

**3.4.1.2 .Water as cooling medium**

The water was circulated to the condenser section and the temperature of water has been varied from 15°C to 30°C, by means of Constant temperature bath. The power input at the evaporator section has been varied from 80W to 100W by means of an autotransformer. Figures 1.21. shows the temperature profile along the heat pipe for power input from 80 to 100W, for a condenser temperature of 30°C and figures 1.22 shows the temperature profile for a condenser temperature of 25°C. Similarly figures 1.23 shows the temperature profile for condenser temperature of 20°C and figures 1.24 shows that for a condenser temperature of 15°C .It was observed that for all cases, the surface temperature of the evaporator reduced for heat pipes charged with the 0.05% and 0.1% vol Al<sub>2</sub>O<sub>3</sub> nanofluid, leading to lower temperature drop between the end of the heat pipe. So, the heat pipe charged with the 0.05% and 0.1% vol Al<sub>2</sub>O<sub>3</sub> nanofluid has good performance than the heat pipe charged with distilled water and 0.01% vol Al<sub>2</sub>O<sub>3</sub> nanofluid.

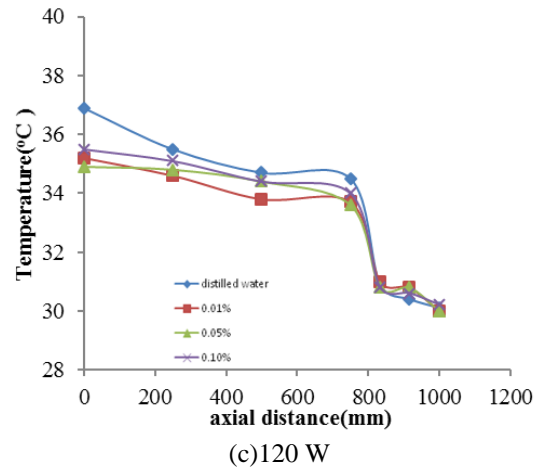
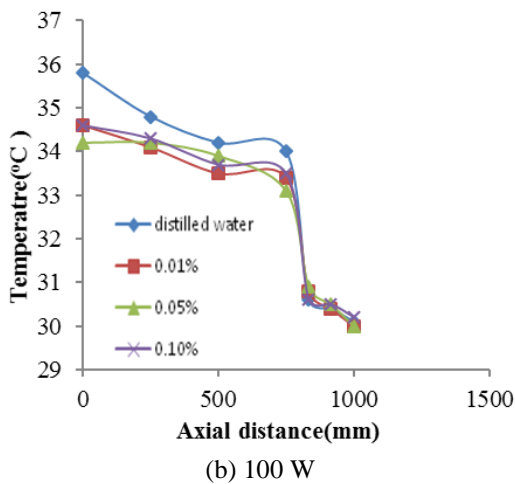
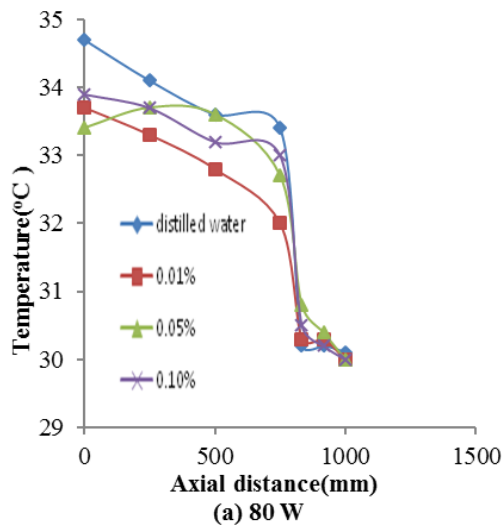
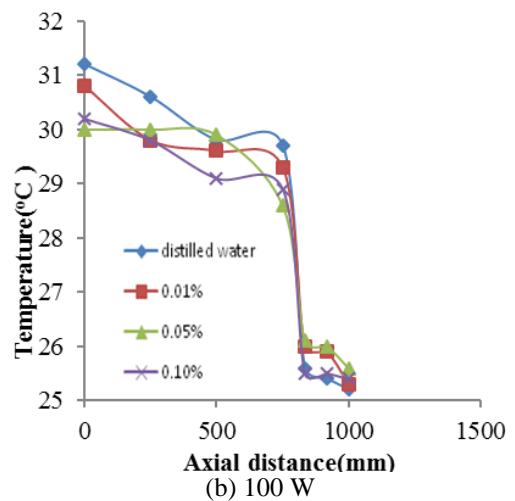
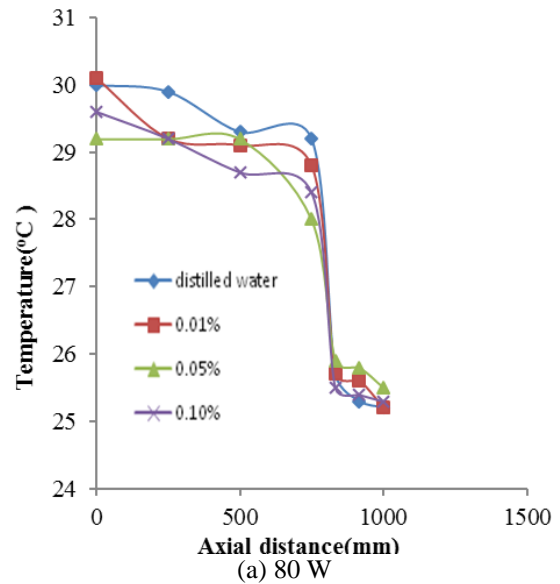


Fig.1.21.Variation of temperature distribution along the heat pipe for the different power input to the evaporator and 30 °C condenser temperature.



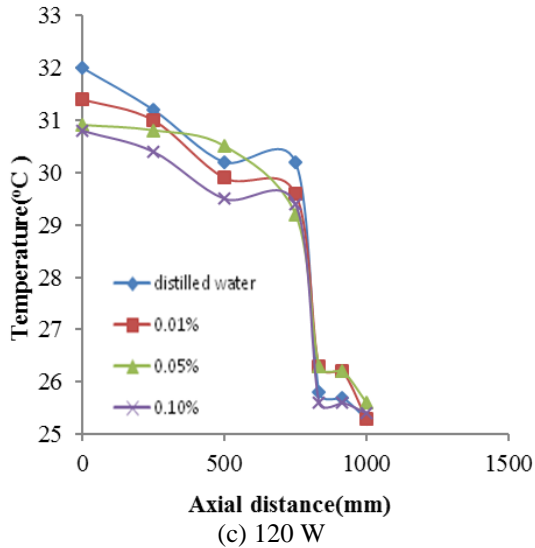


Fig.1.22. Variation of temperature distribution along the heat pipe for the different power input to the evaporator and 25 °C condenser temperature.

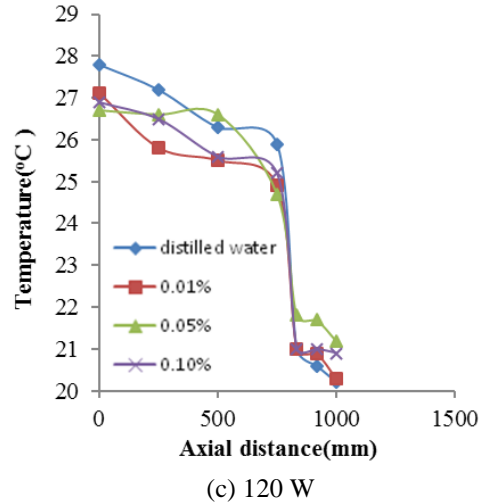
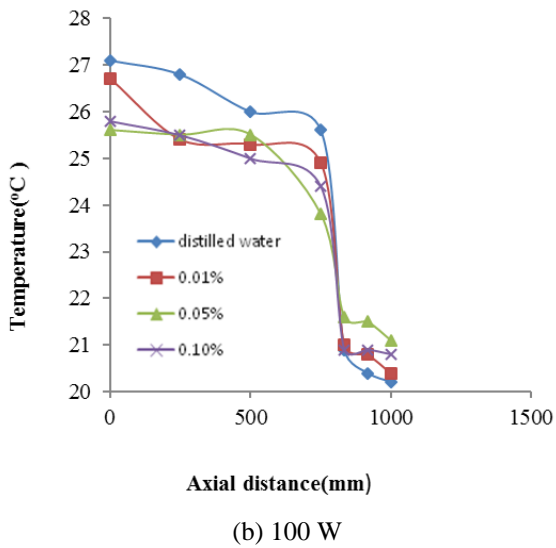
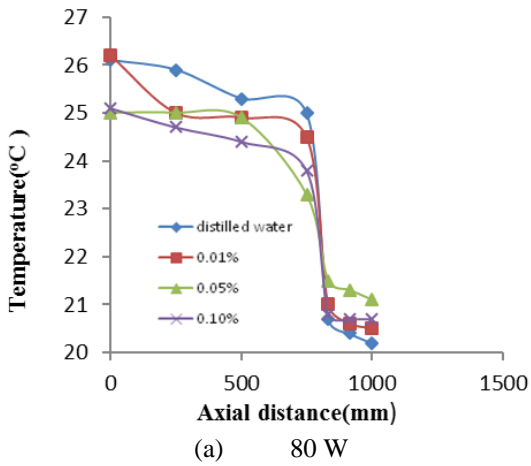
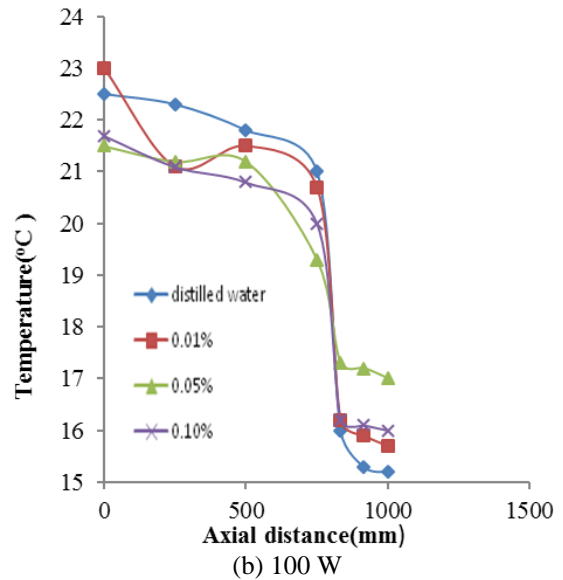
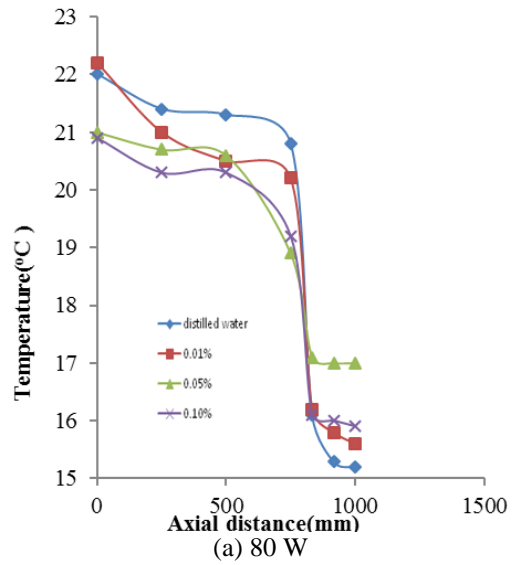


Fig.1.23. Variation of temperature distribution along the heat pipe for the power input to the evaporator and 20 °C condenser temperature.



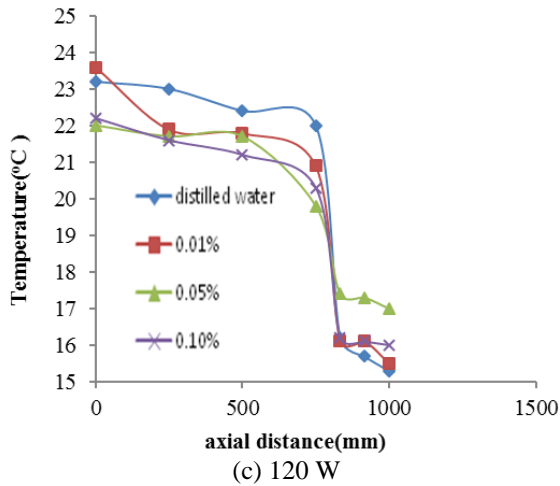


Fig.1.24. Variation of temperature distribution along the heat pipe for the power Input to the evaporator and 15 °C condenser temperature.

**3.4.2. Thermal conductance**

Thermal conductance is the quantity of heat that passes in unit time through particular area and thickness, when its opposite faces differ in temperature by one Kelvin and it is obtained by dividing the heat input by the average temperature difference between condenser and evaporator as,

$$\text{Thermal conductance} = \frac{Q}{T_{avg\,evap} - T_{avg\,cond}} \quad (1.3)$$

The thermal conductance of the heat pipe for the various operating condition is shown in the figures 1.25 to 1.29. Thermal conductance was observed to increase with the increase in power input at the evaporator section. Fig. 1.25 shows the variation of thermal conductance of heat pipe with the power input to the evaporator without circulating the water in the condenser, which shows that the thermal conductance of the heat pipe charged with the 0.05% and 0.1% vol Al<sub>2</sub>O<sub>3</sub> nanofluid is more than the heat pipe charged with the distilled water and 0.01% vol Al<sub>2</sub>O<sub>3</sub> nanofluid. Also thermal conductance of the heat pipe charged with the 0.05% vol Al<sub>2</sub>O<sub>3</sub> nanofluid is 2.5 times the thermal conductance of the heat pipe charged with the distilled water and 0.01% vol Al<sub>2</sub>O<sub>3</sub> nanofluid. Figures 1.26 to 1.29 shows the variation of thermal conductance of heat pipe with the power input to the evaporator, circulating the water in the condenser at temperature, ranging from 15 to 30°C, with an interval of 5°C. The thermal conductance of the heat pipe charged with the 0.01%, 0.05% and 0.1% vol Al<sub>2</sub>O<sub>3</sub> nanofluid is greater than the heat pipe charged with the distilled water and thermal conductance of the heat pipe charged with the 0.05% vol Al<sub>2</sub>O<sub>3</sub> nanofluid is 1.3 times greater than the thermal conductance of the heat pipe charged with the distilled water for the case when the water is circulated to the condenser at 30 °C, as shown in fig.1.26. Figures 1.27 to 1.29 also shows that heat pipe charged with the 0.05% vol Al<sub>2</sub>O<sub>3</sub> nanofluid has higher thermal conductance than the other heat pipes.

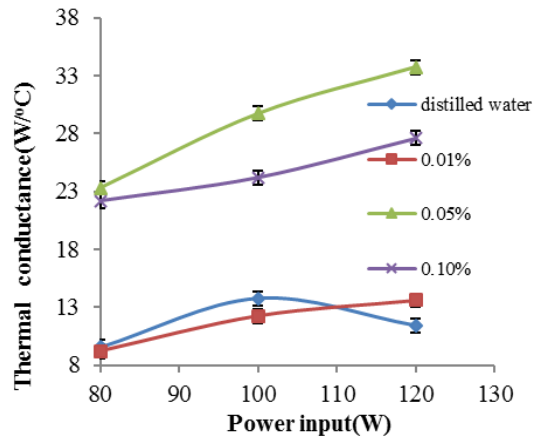


Fig.1.25. Variation of thermal conductance of heat pipe with the power input to the evaporator without circulating the water to the condenser.

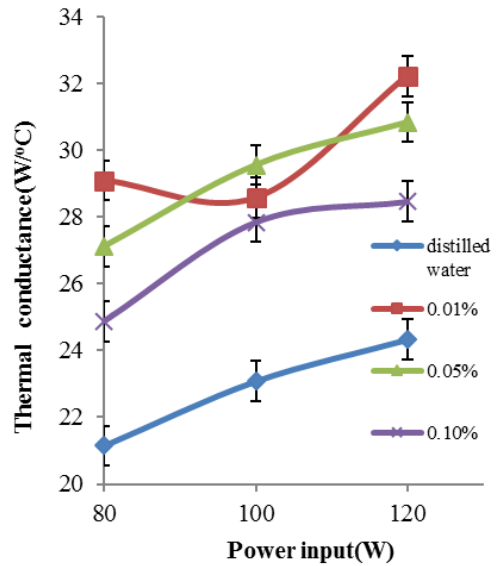


Fig.1.26. Variation of thermal conductance of heat pipe with the power input to the evaporator with circulating the water to the condenser at 30 °C.

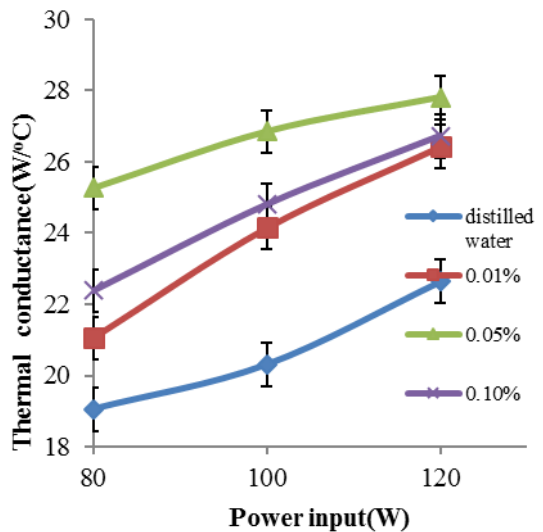


Fig.1.27. Variation of thermal conductance of heat pipe with the power input to the evaporator with circulating the water to the condenser at 25 °C.

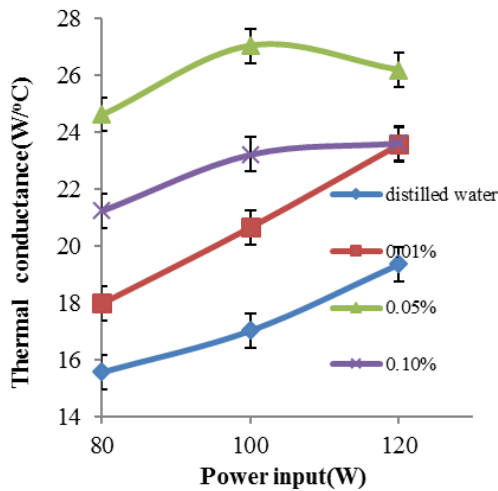


Fig.1.28. Variation of thermal conductance of heat pipe with the power input to the evaporator with circulating the water to the condenser at 20 °C.

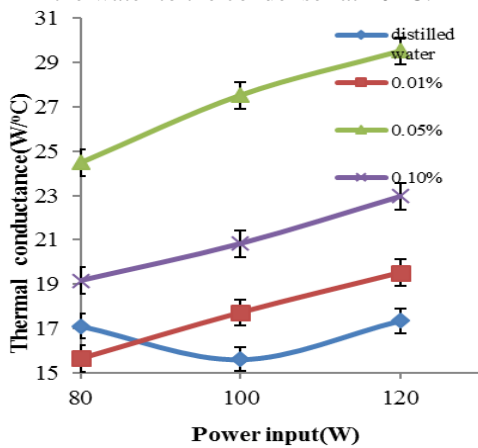


Fig.1.29. Variation of thermal conductance of heat pipe with the power input to the evaporator with circulating the water to the condenser at 15 °C.

**3.4.3. Effective thermal conductivity**

Effective thermal conductivity is a performance indicator that helps to compare various designs of the heat pipes. The effective thermal conductivity is defined on the basis of the Fourier’s law of heat conduction as follows:

$$k_{eff} = \frac{Q}{A_c \frac{\Delta T}{L}} \tag{1.4}$$

The above equation essentially compares the heat transfer in the heat pipe, with that in a solid conductor, to obtain an effective value of thermal conductivity. From equation it is obvious that the effective thermal conductivity is inversely proportional to the temperature difference between the extreme ends of the heat pipe (terminal temperature drop), for a given heat input. A large value of the effective thermal conductivity indicates that the heat pipe operates close to isothermal, for a given heat transport. The effective thermal conductivity of the heat pipe for the various operating condition is shown in the figures 1.30 to 1.34. The effective thermal conductivity increases as the power input to the evaporator increases. Fig. 1.30 shows the

variation of effective thermal conductivity of heat pipe with the power input in the evaporator section, without circulating the water in the condenser. The effective thermal conductivity of the heat pipe charged with the 0.05% vol Al<sub>2</sub>O<sub>3</sub> nanofluid was found to be 2.5 times than that of the heat pipe charged with the distilled water. Figures 1.31 to 1.34 shows the variation of thermal conductance of heat pipe with the power input of the evaporator, while circulating water in the condenser at temperatures ranging from 15 to 30°C, with an interval of 5°C. The thermal conductance of the heat pipe charged with the 0.01%, 0.05% and 0.1% vol Al<sub>2</sub>O<sub>3</sub> nanofluid is greater than the heat pipe charged with the distilled water and effective thermal conductivity of the heat pipe charged with the 0.05% vol Al<sub>2</sub>O<sub>3</sub> nanofluid is 1.35 times greater than the effective thermal conductivity of the heat pipe charged with the distilled water for the case when the water is circulated in the condenser at 30 °C.

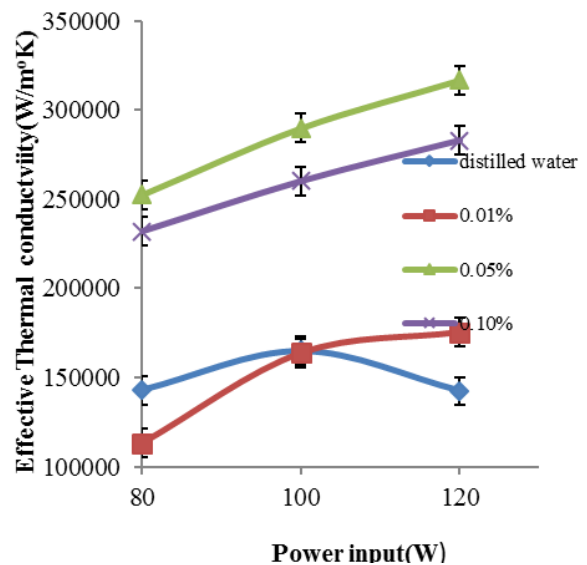


Fig.1.30. Variation of effective thermal conductivity of heat pipe with the power input to the evaporator without circulating the water to the condenser.

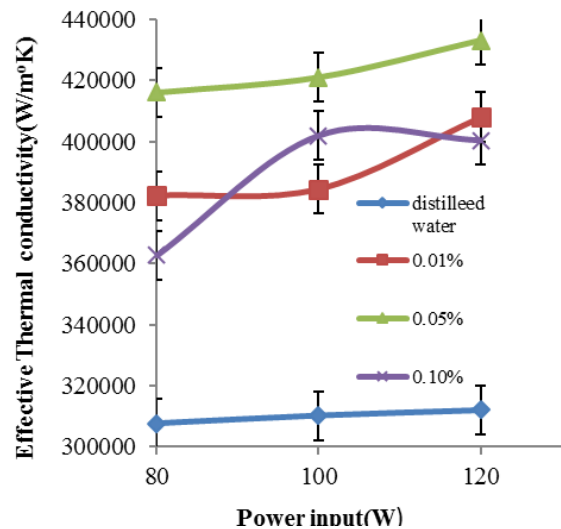




Fig.1.31. Variation of effective thermal conductivity of heat pipe with the power input to the evaporator with circulating the water to the condenser at 30 °C.

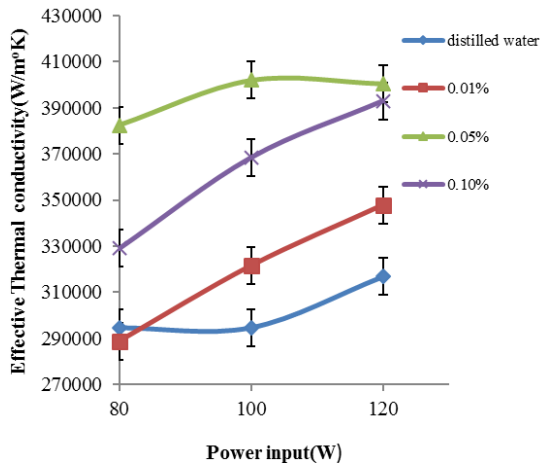


Fig.1.32. Variation of effective thermal conductivity of heat pipe with the power input to the evaporator with circulating the water to the condenser at 25 °C.

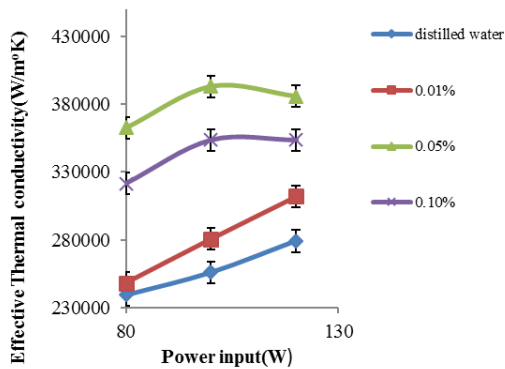


Fig.1.33. Variation of effective thermal conductivity of heat pipe with the power input to the evaporator with circulating the water to the condenser at 20 °C.

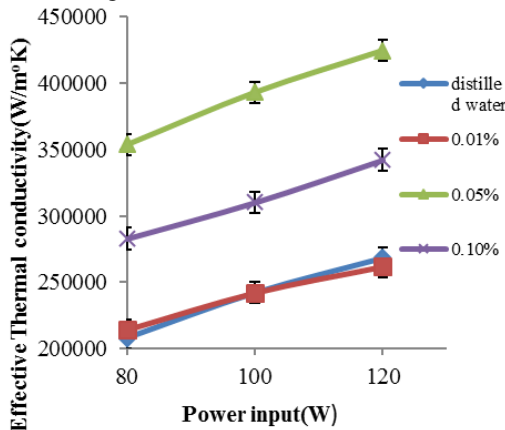


Fig.1.34. Variation of effective thermal conductivity of heat pipe with the power input to the evaporator with circulating the water to the condenser at 15 °C.

**3.4.4 Uncertainty analysis**

The uncertainty analysis was done to estimate the uncertainty in the measurement values for the experiments conducted. The uncertainty in the thermocouple measurement is ±0.5 °C and that in input

power is ±0.01W. The uncertainty in the measurement of Thermal conductance was estimated to be ±0.5 W/°C or 6% and that in the measurement of effective thermal conductivity is ± 8000 W/m²K or 5%.

**3.4.5 Wick analysis**

After the extensive experimentation, heat pipe has been cut out to investigate the possibility of deposition of Al<sub>2</sub>O<sub>3</sub> nanoparticle on the wick structure. Al<sub>2</sub>O<sub>3</sub> nanofluid of 0.05% vol concentration, before charging and after the experimentation in the heat pipe is shown in fig.1.35. The color of the sample has been changed to yellow-brownish color, which may be due to the reaction of copper wick with the Al<sub>2</sub>O<sub>3</sub> nanofluid or may be due to presence of some rust or dust present inside the heat pipe, during the charging process. The cross sectional view of the heat pipe charged with 0.05% vol Al<sub>2</sub>O<sub>3</sub> nanofluid is shown in fig.1.36.



Fig.1.35. 0.05% vol Al<sub>2</sub>O<sub>3</sub> nanofluid before and after the operation of heat pipe.

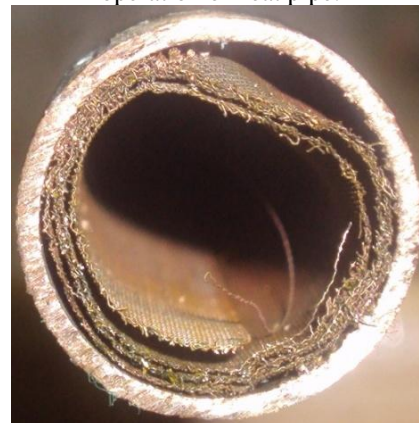


Fig.1.36. Cross sectional view of the wick of heat pipe

Heat pipe charged with 0.05% vol. Al<sub>2</sub>O<sub>3</sub> nanofluid EDS was taken for the wick structure of the heat pipe which was charged with 0.05% vol Al<sub>2</sub>O<sub>3</sub> nanofluid to investigate the presence of nanoparticles in the wick structure. The weight and atomic percentage of each component present in the wick structure is shown in Table .1. The scanned area of the wick structure, for the EDS analysis is shown in fig.1.37. The EDS spectrum of the Al<sub>2</sub>O<sub>3</sub> nanoparticle (fig.1.38) confirms the presence of Al<sub>2</sub>O<sub>3</sub> nanoparticle.

Table.1.Weight and Atomic percentage of elements present in the wick structure from EDS data

Element	Weight %	Atomic %
O (K)	30.16	60.78
Al (K)	5.52	6.59
Cu(L)	64.32	32.63
Total	100	

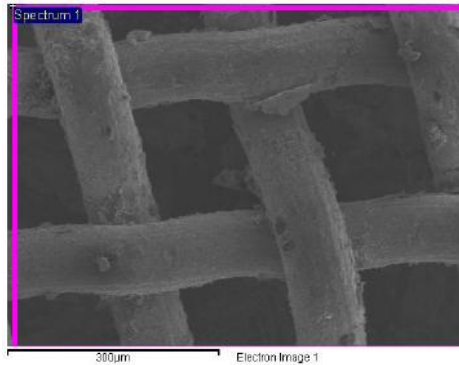


Fig.1.37.Scanned area images of wick structure

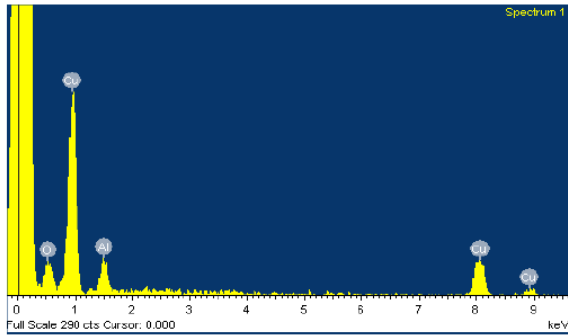


Fig.1.38. EDS spectrum of wick structure of heat pipe for EDS analysis of heat pipe charged with 0.05% vol $\text{Al}_2\text{O}_3$  nanofluid.

The SEM images of the wick structure of the heat pipe charged with distilled water and 0.05% vol  $\text{Al}_2\text{O}_3$  nanofluid are shown in the fig.1.39 and fig.1.40. Fig.1.40. confirms the deposition of  $\text{Al}_2\text{O}_3$  nanoparticle on the wick structure and it also shows the blockage of these nanoparticles in the pores, which may affect the performance of heat pipe, in long run.

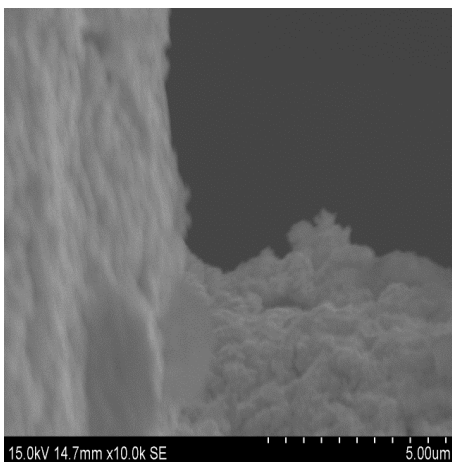


Fig.1.39.SEM image of wick of heat pipe charged with distilled water

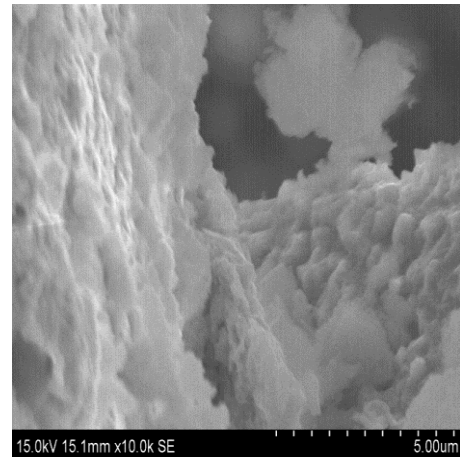


Fig.1.40.SEM image of wick of heat pipe charged with 0.05% vol $\text{Al}_2\text{O}_3$  nanofluid

#### IV. CONCLUSIONS

Heat pipe is an efficient heat transfer device which has several application in electronic cooling, solar heat recovery system and spacecraft thermal management etc. The performance of thermo-physical properties of working fluids influences the performance of the heat pipe. The present work aims at the experimental investigation on the possibility of use of dilute nano fluids as working fluid in heat pipes, which is used for the solar applications. Various thermo physical properties of  $\text{Al}_2\text{O}_3$  nanofluid and distilled water such as surface tension, thermal conductivity and Dynamic viscosity by using standard methods and instruments have been determined. Experimental methods have been employed to determine the properties of the wick structure such as capillary pressure and permeability using  $\text{Al}_2\text{O}_3$  nanofluid and distilled water. The heat pipe was designed based on the solar water heating application and four heat pipes were fabricated and charged with distilled water and three different concentration of  $\text{Al}_2\text{O}_3$  nanofluid. The performance of the heat pipes was tested experimentally by using the setup developed in the laboratory. The wick was analyzed after the experiment by to find out the possibility of deposition nanoparticle in the wick structure.

Following are some of the conclusions drawn from the present work,

- 1) The surface tension of the  $\text{Al}_2\text{O}_3$  nanofluids was found to be increase as compared to distilled water. So, all the limits values such as capillary limit, entrainment limit and boiling limit of the heat pipe will increase correspondingly.
- 2) The thermal conductivity of the  $\text{Al}_2\text{O}_3$  nanofluids increases as the concentration increases, which in turn increase the boiling limit of the heat pipe.
- 3) The dynamic viscosity of the  $\text{Al}_2\text{O}_3$  nanofluids increases with the concentration of nanoparticles and found to decrease with the temperature, which will decrease the capillary limit of the heat pipe.

4) The capillary pressure of the  $\text{Al}_2\text{O}_3$  nanofluid increases with the concentration, which will improve the capillary action of the wick structure compared with the distilled water.

5) The permeability of wick structure with the nanofluid decreases, which will affect the flow of nanofluid inside the wick structure.

6) The temperature drop at the both the ends of the heat pipe was observed to be reduce by 6 - 7 °C for the heat pipe charged with 0.05% and 0.1% vol  $\text{Al}_2\text{O}_3$  nanofluid as compared with the heat pipe charged with the distilled water and 0.01% vol  $\text{Al}_2\text{O}_3$  nanofluid, when the water is not circulated in the condenser.

7) When the water is circulated at different temperature and the different power input the surface temperature of the heat pipe at the evaporator section charged with 0.05% and 0.1% vol  $\text{Al}_2\text{O}_3$  nanofluid got reduced.

8) The thermal conductance and the effective thermal conductivity of the 0.05%  $\text{Al}_2\text{O}_3$  nanofluid charged heat pipe was found to be 1.3 and 1.35 times greater than the heat pipe charged with distilled water.

9) Presence of the nanoparticles in the wick structure after experimentation of heat pipe was confirmed with the help of SEM images.

#### SCOPE FOR FUTURE WORK

1) The carbon nanotube CNT or fullerene can be added to the working fluid since this nanoparticle has higher thermal conductivity and this nanofluid can be used in the heat pipe.

2) The wick can be coated with the nanoparticle this may increase the capillary action since this may affect the wetting characteristic of the fluid with the wick structure.

3) The pore size of the wick structure can be reduced to nanosize so that the capillary action will be more effective.

#### REFERENCES

- [1] D.A. Reay and P.A. Kew: Heat Pipe-Theory Design and Application, 5<sup>th</sup> edition 2006, Elsevier publication.
- [2] Chi S W: Heat Pipe Theory and Practice: McGraw-Hill Publishing Company, New York, NY, 1976.
- [3] K. N. Shukla: Thermal Performance of Cylindrical HeatPipe Using Nanofluids, Journal of thermophysics and heat transfer, Vol. 24, No. 4, 2010, pp 796-802.
- [4] M. G. Mousa: Effect of Nanofluid Concentration on the Performance of Circular Heat Pipe, International Journal of Scientific & Engineering Research Volume 2, Issue 4, 2011.
- [5] Shung-Wen Kang, Wei-Chiang Wei, Sheng-Hong Tsai and Chia-Ching Huang: Experimental investigation of nanofluids on sintered heat pipe thermal performance, Applied Thermal Engineering 29, 2009, pp 973–979.
- [6] Shung-Wen Kang, Wei-Chiang Wei, Sheng-Hong Tsai and Shih-Yu Yang: Experimental investigation of silver nano-fluid on heat pipe thermal performance, Applied Thermal Engineering 26, 2006, pp 2377–2382.
- [7] KyuHyung Do, Hyo Jun Ha and SeokPil Jang: Thermal resistance of screen mesh wick heat pipes using the water-based  $\text{Al}_2\text{O}_3$  nanofluids, International Journal of Heat and Mass Transfer 53, 2010, pp 5888–5894.
- [8] ZhenHuaLiu and QunZhiZhu: Application of aqueous nanofluids in a horizontal mesh heat pipe,Energy Conversion and Management 52 ,2011, pp 292–300.
- [9] Maryam Shafahi, Vincenzo Bianco , Kambiz Vafai, and Oronzio Manca: Thermal performance of flat-shaped heat pipes using nanofluids, International Journal of Heat and Mass Transfer 53,2010,pp 1438-1445.
- [10] Gabriela Huminic , Angel Huminic , Ion Morjanand Florian Dumitrache: Experimental study of the thermal performance of thermosyphon heat pipe using iron oxide nanoparticles, International Journal of Heat and Mass Transfer 54, 2011, pp 656- 661.
- [11] E. Azad: Performance analysis of wick-assisted heat pipe solar collector and comparison with experimental results, Heat Mass Transfer (2009) 45 pp 645–649.
- [12] Hassam Nasarullah Chaudhrya, Ben Richard Hughesa and Saud Abdul Ghani: A review of heat pipe systems for heat recovery and renewable energy applications, Renewable and Sustainable Energy Reviews 16 (2012), pp 2249–2259.
- [13] Lin Lu, Zhen-Hua Liu and Hong-Sheng Xiao:Thermal performance of an open thermosyphon using nanofluidsfor high-temperature evacuated tubular solar collectors Part 1: Indoor experiment, Solar Energy 85 (2011),pp 379–387.
- [14] RaminHajian ,Mohammad Layeghi and Kamal Abbaspour Sani: Experimental study of nanofluid effects on the thermal performance with response time of heat pipe,Energy Conversion and Management 56 (2012),pp 63–68.
- [15] Gopalan Ramesh and Narayan Kotekar Prabhu: Review of thermo-physical properties, wetting and heat transfer characteristics of nanofluids and

their applicability in industrial quench heat treatment, Nanoscale Research Letters 2011.

[16] G. Harish, V. Emlin, V. Sajith: Effect of surface particle interactions during pool boiling of

nanofluids, International Journal of Thermal Sciences xxx 2011.

[17] Dr. C Robert Samuel: Heat pipe application for dissipating heat from the equipment bay for remote piloted vehicles', 1991.

